

The Role of Long-Period Ground Motions on Magnitude and Damage of Volcanic Earthquakes on Mt. Etna, Italy

by Giuliano Milana, Antonio Rovelli, Adriano De Sortis, Giovanna Calderoni, Giuseppe Coco, Mauro Corrao, and Paolo Marsan

Abstract On October 2002, a seismic swarm occurred on Mt. Etna. One of the strongest events caused severe damage, up to a European Macroseismic Scale intensity of VIII that contrasts with its local magnitude of 4.4. The occurrence of significant damage at such a small magnitude is repeatedly observed in the area and is traditionally attributed to shallow source. Recorded strong-motion accelerograms and broadband seismograms demonstrate that there is one more cause for the severe damage, that is, an anomalously strong low-frequency ($0.1 < f < 1$ Hz) radiation deviating from the conventional Brune (1970) spectral scaling. Therefore, these earthquakes cause large ground displacements and long (≈ 20 sec) durations of shaking. The integration of digital accelerograms yields a maximum peak ground displacement as large as 1.8 cm at a distance of 18 km. Based on the sharp local attenuation of ground motion in the study area, we infer that peak ground displacements near the epicenters did exceed 10 cm. The occurrence of large displacements caused selective damage to medium-rise (≥ 3 stories) reinforced concrete buildings and elements like church façades.

The frequency cutoff below 1.25 Hz in the Wood–Anderson response attenuates the peak-to-peak amplitudes used to assess local magnitudes. Therefore, M_L values are not representative of the real strength of volcanic earthquakes. Because a prompt magnitude (and damage potential) assessment is crucial for civil protection actions, a procedure is proposed which, in near-real time, can be successful in identifying potentially damaging earthquakes of Mt. Etna through the computation of pseudoveLOCITY response spectra. The procedure provides a magnitude value that is derived on a statistical basis from the Housner (1952) spectral intensity computed in the low-frequency band. This parameter is a suitable near-real-time indicator of large earthquake-induced building shaking and could also be applied for a preliminary estimate of the epicentral macroseismic intensity.

Introduction

Between 26 and 29 October 2002, the Mt. Etna area was intensely struck by several earthquakes widely felt by the population in a large area of eastern Sicily, from Messina to Siracusa (Fig. 1). These shocks were part of a seismic swarm consisting of some hundred events in the first four days of activity and lasting up until early 2003. Earthquakes were located in two separate areas of Mt. Etna (Fig. 1), as described by Barberi *et al.* (2004) and Patanè *et al.* (2006). A first group of epicenters is located in the east-northeast part of the volcano, reaching a maximum local magnitude of 4.6 on October 27 at 02:50 coordinated universal time (UTC). The second group, occurring after October 28, was located in the southeast flank close to the town of Zafferana Etnea and culminated with the M_L 4.4 earthquake of October 29 at

10:02 UTC (Fig. 1). The seismic swarm coincided with the reactivation of the eruptive fracture system originated by the 2001 eruption. The strongest events, along with their magnitudes, are listed in Table 1.

The most damaging event was the M_L 4.4 earthquake of October 29 (event 4 in Table 1), which occurred in a densely urbanized area and attained intensity VIII of the European Macroseismic Scale (EMS, see Grunthal, 1998). In spite of its small local magnitude, the shock caused significant damage to many buildings, including reinforced concrete ones (Fig. 2a,b,c), in an area that extends for about 4 km in a north-northwest–south-southeast direction and is centered around the villages of Santa Venerina and Guardia (Azzaro, D’Amico, *et al.*, 2006). A long system of surface

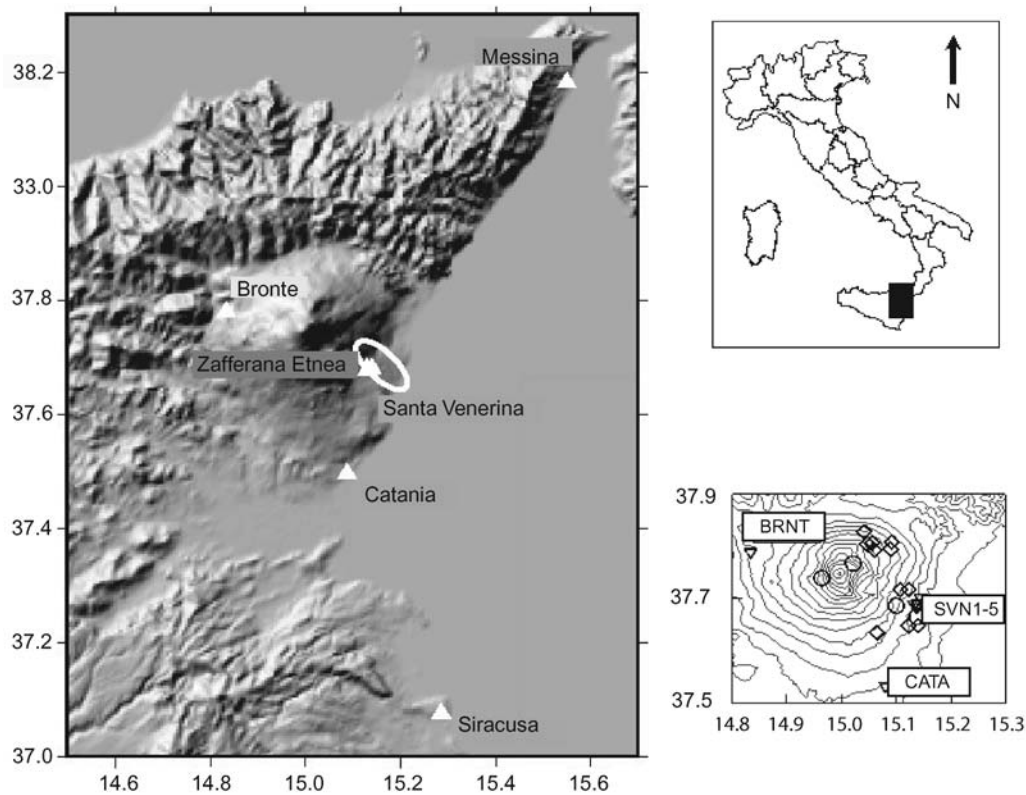


Figure 1. Map of the study area. The zone of the largest damage, including the village of Santa Venerina, is elongated northwest–southeast (left-hand panel). In the right-hand bottom panel, open circles are the strongest events of the swarm, recorded at the accelerometric stations CATA and BRNT; diamonds are later, minor events recorded by temporary stations SVN1 to SVN5.

fractures occurred in the damaged area. Other similar and even stronger events (e.g., event 3 in Table 1) in the northern zone did not cause diffuse damage because they occurred in a

sparingly populated area; however, the level of destruction was high for the few sparse buildings close to the epicenters (Fig. 2d).

Table 1
List of the Events Used in the Present Study

Event Number	Date (yyyy/mm/dd)	Time (hr:min:sec)	Latitude (°)	Longitude (°)	M_w Mednet	M_L Mednet	M_L (this work)	Recording Stations
1	2002/10/27	01:28:17.59	37.808	15.051			4.3	B
2	2002/10/27	01:58:11.23	37.740	14.964			4.6	B
3	2002/10/27	02:50:25.01	37.768	15.021	4.9	4.6	4.7	B, C
4	2002/10/29	10:02:20.23	37.687	15.100	4.7	4.4	4.8	C
5	2002/10/29	16:39:46.78	37.666	15.138	4.2	4.1	4.4	C
6	2002/12/03	13:50:27.00	37.795	15.089			2.7	1
7	2002/12/03	21:07:59.00	37.648	15.122			3.2	1, 2, 3, 4
8	2002/12/04	05:17:25.00	37.649	15.139			3.0	1, 2, 3, 4
9	2002/12/04	13:16:33.00	37.718	15.123			3.4	1, 2, 3, 4, 5
10	2002/12/05	22:59:57.00	37.794	15.060			3.0	1, 2, 3, 4, 5
11	2002/12/24	01:12:59.00	37.807	15.056			3.7	4, 5
12	2002/12/24	13:32:09.00	37.805	15.047			2.4	5
13	2002/12/27	10:37:17.00	37.809	15.091			3.1	5
14	2002/12/28	08:24:22.00	37.829	15.041			2.5	5
15	2003/01/19	00:34:59.00	37.718	15.107			2.7	4
16	2003/01/25	03:29:20.00	37.636	15.065			2.2	2, 3, 4

Station codes B and C refer to BRNT and CATA, respectively; the numbers indicate stations SVN1 to SVN5. Epicentral coordinates are provided by the INGV-Catania team (courtesy of Domenico Patanè). Local magnitudes of this work are synthesized from the available local recordings.

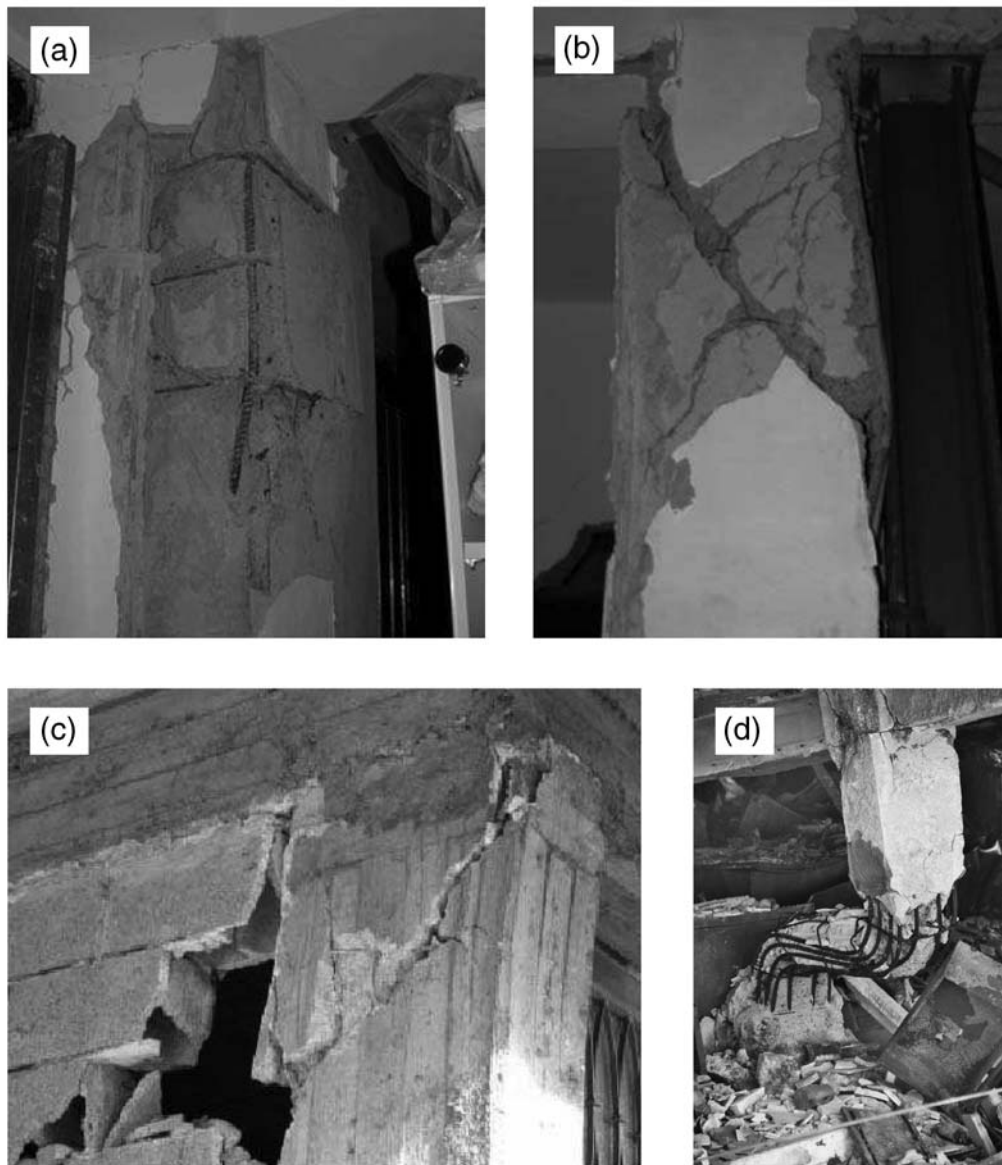


Figure 2. Example of damaged three- and four-story buildings in the epicentral area of (a), (b), and (c) during the M_L 4.4 earthquake of 29 October 2002 and (d) the M_L 4.6 earthquake of 27 October 2002.

The cue to this study was the discrepancy between the observed level of damage, confirmed by the statistical elaboration of buildings' survey data, and the small magnitude of the October 2002 swarm. These volcanic earthquakes were the first destructive events to be recorded locally on scale on high resolution digital instruments. Their recordings offer the opportunity of analyzing the spectral content of the volcanic events of Mt. Etna down to frequencies of about 0.1 Hz that were never investigated thus far. In this study, we document to what extent the volcanic earthquakes of October 2002 deviate from the conventional source scaling of tectonic earthquakes, attaining much larger amplitudes in the low-frequency band. Thus, we demonstrate that shallow source or permanent deformations can be possible concomitant causes

for the large damage produced by volcanic earthquakes of Mt. Etna, but there are more cogent factors intrinsically connected to the special spectral structure of these events. We also introduce a new criterion to discriminate potentially damaging volcanic earthquakes in near-real time.

Data

The data used in this study are strong-motion accelerograms recorded at Catania (CATA) and Bronte (BRNT) as well as broadband seismograms of five temporary stations (SVN1 to SVN5) deployed in the Santa Venerina territory to record small events (Fig. 1). The strong-motion stations CATA and BRNT belong to the Italian Accelerometric Net-

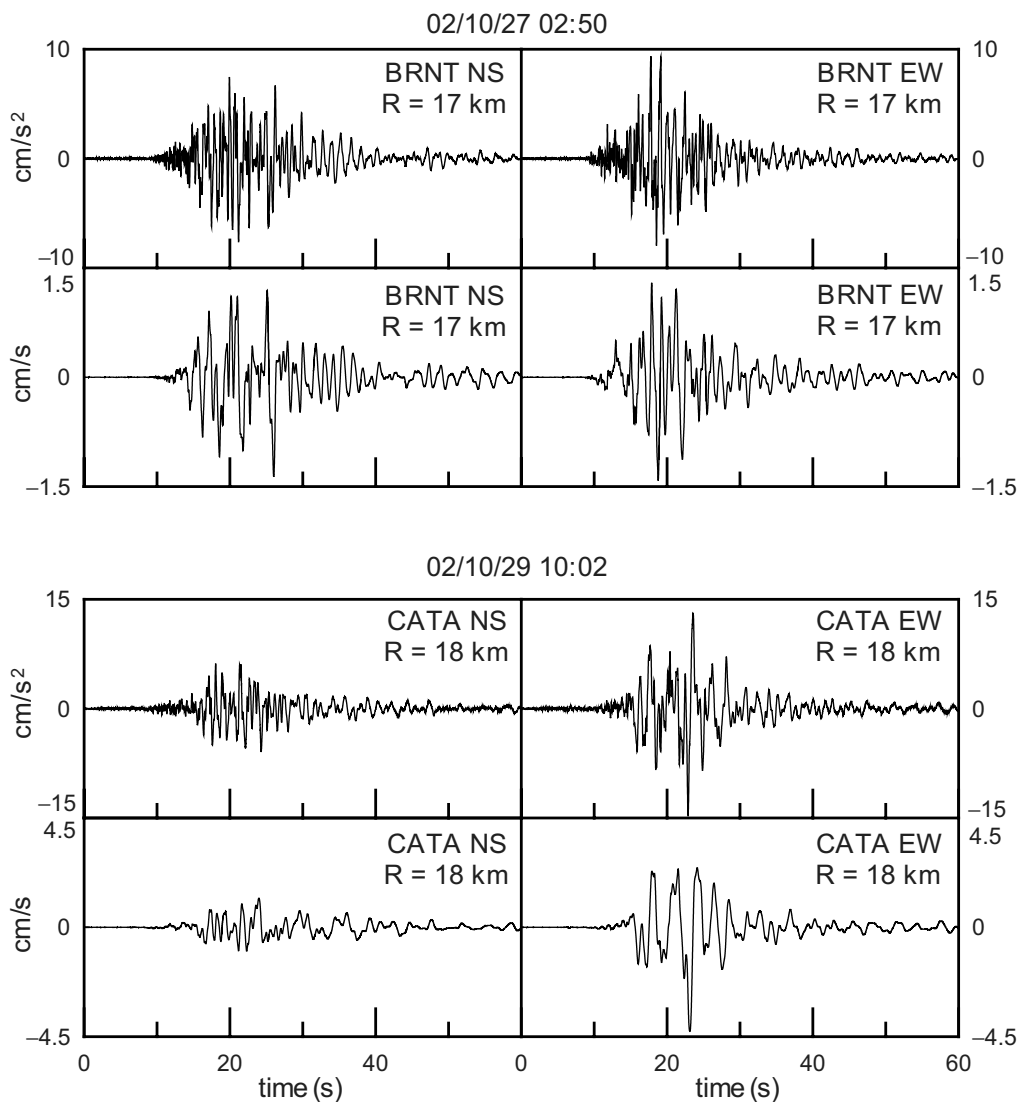


Figure 3. Specimens of ground accelerations and velocities of events of the October 2002 swarm.

work owned by the Dipartimento Protezione Civile of Italy. These stations are equipped with Kinematics model Etna digitizers and Episensor accelerometers. The full scale is set to $1g$, and data were recorded in trigger mode with an activation threshold of 3 gal on any of the three components. The sampling rate was 200 samples/sec.

The broadband seismological stations, equipped with three-component Guralp CMG-40T seismometers and Ref-Tek 72A digitizers, were installed in the Santa Venerina area beginning on 3 December 2002. They operated up to 25 January 2003 in a continuous recording mode with a sampling rate of 125 samples/sec and recorded late events of the swarm up to a maximum local magnitude of 3.7.

Magnitudes of the swarm events are computed from recordings at local and regional distances. Moment magnitudes (M_w) are available only for three of the events that triggered accelerographs. Their values can be found in the catalog of

Regional Centroid Moment Tensor (RCMT) determinations (Pondrelli *et al.*, 2004). For the same events, the MedNet catalog available at <http://mednet.rm.ingv.it/> (last accessed in May 2008) also provides local magnitudes M_L obtained through the Wood–Anderson numerical synthesis of broadband seismograms of the MedNet stations, applying the conventional distance correction (Richter, 1958). For the events of October 2002 not included in the MedNet catalog of local magnitudes, we have generated synthetic Wood–Anderson seismograms using the strong-motion accelerographs of CATA and BRNT. These M_L values tend to overestimate those of the MedNet catalog when both are available. The same procedure was also adopted for events occurring after 3 December 2002 using the local records of stations SVN1 to SVN5. The list of earthquakes used in the analysis and their magnitude estimates are shown in Table 1.

Ground-Motion Analysis

Strong Motions

The pattern of activation of the two strong-motion stations reflects the temporal and spatial evolution of the swarm. The accelerometer of BRNT, which is closer to the epicenters in the east-northeast part of Mt. Etna, was triggered by three of the events of October 27 occurring in that area. The M_L 4.6 event of October 27 (event 3) is the only one that triggered both BRNT and CATA. The accelerometer of CATA, which is closer to the southeast flank of Mt. Etna, was also triggered by two of the events of October 29 (events 4 and 5) occurring in the Santa Venerina area (Table 1). The ground-motion waveforms of these earthquakes (specimens are shown in Fig. 3) indicate a long (≈ 20 sec) duration along with a predominance of low frequencies. Such features are commonly observed in volcanic areas as also documented by Jousset and Douglas (2007) and references therein.

Horizontal peak ground acceleration (PGA) and velocity (PGV) of the October 2002 swarm deviate from the statistical expectations of the Sabetta and Pugliese (1987) regression (hereafter denoted as SP87) computed on the Italian strong-motion data (Table 2). This comparison is made only to give a first idea about the anomaly of the recorded events, in full awareness that it is not strictly appropriate for two reasons. First, the attenuation relationships were assessed by SP87 using earthquakes in Italy with magnitude > 4.6 and should not be used for smaller magnitudes. Second, the authors did not include earthquakes of volcanic areas in their analysis and therefore their attenuation law is not intended for them. Nevertheless, we believe that this comparison is useful to stress the inadequacy, for volcanic events, of commonly adopted ground-motion scaling laws in Italy. This is especially important for the hazard assessment in the Mt. Etna area. Another comparison can be done using a new attenuation law assessed for smaller magnitude events by Bragato and Slejko (2005) (hereafter referred to as BS05) that reduces the risk of overestimating ground motion for events with magnitudes lower than 5.5. However, this attenuation law is not estimated for volcanic earthquakes. We also checked the ShakeMap regression (WA05 hereafter) for small events, derived from Wald *et al.* (1999) extending to 2002 the event database (Wald *et al.*, 2005).

Figure 4 shows the comparison between observed and expected PGAs and PGVs. Compared to SP87, recorded PGAs are always smaller than predicted, whereas recorded PGVs are more consistent with predicted ones. The use of BS05 attenuation law gives smaller overestimates of PGA, but PGV values are significantly underpredicted. WA05 tends to fit ground accelerations but completely fails in predicting ground velocities. Note that the earthquake causing the most damage (event 4) largely exceeds the PGV prediction of all the attenuation laws. Figure 4 indicates that none of the commonly used attenuation laws can simultaneously fit PGA and PGV values, and the spectral analysis of records explains this

distinctive feature of volcanic events. Figure 5a–e compares the Fourier amplitude spectra of the accelerograms to the Brune (1970) spectra expected for the moment magnitude and source-to-receiver distance of the events. Theoretical spectra of Figure 5 are modeled through the attenuation law inferred from eastern Sicily tectonic earthquakes by Scognamiglio *et al.* (2005). The evident deviation from the conventional scaling of tectonic earthquakes is therefore the origin of the anomalously small accelerations of volcanic events of the October 2002 swarm. Acceleration spectra of CATA show a significant depletion in the high-frequency amplitude and a large spectral bump in the frequency band 0.1–1 Hz. Also, station BRNT has the same tendency, although there is a better fit of high frequencies, and the exaggeration of low-frequency amplitudes has a smaller extent. The difference in the spectral bump between BRNT and CATA for the same event (Fig. 5a,c) could erroneously lead to the conclusion that CATA is affected by a site effect. However, this interpretation has to be ruled out because the same station shows no amplification at low frequency in the spectra of tectonic events (a specimen of an Hyblean Mounts event is shown in Fig. 5f).

Both BRNT and CATA are installed on the volcanic edifice of Mt. Etna. Two broadband stations of MedNet (namely AIO and VAE, around 30–35 and 50–55 km, respectively, from the epicenters) also recorded the sequence on scale. Their records confirm the spectral increment in the 0.1–1 Hz frequency band but show strongly attenuated amplitudes. However, their ground displacement amplitudes agree with those reported by Jousset and Douglas (2007) at similar epicentral distances and magnitudes. A possible explanation could be that the same attenuation model cannot be applied inside and outside the volcanic edifice; for this reason, AIO and VAE were not used in the analysis.

For the strongest events of October 2002, the double integration of the digital accelerograms yields ground displacements of about 1.8 cm at a distance of 18 km (Fig. 6d). Records were baseline corrected and integrated following the Boore and Bommer (2005) procedure. Attenuation of ground displacement of the Mt. Etna area is typically very sharp within the first 20 km from the epicenter. This is well documented by data recorded during the M_L 3.5 earthquake of 31 October 2005 (Fig. 6e) when the PGD recorded at CATA (black diamond) decreased by more than a factor of 10 compared to the closest station. Starting from this observation, we infer that horizontal ground displacement could have attained amplitudes as large as 15 cm in the epicentral area during the October 29 (event 4) event. A sharp amplitude decay within the first 20 km is also expected, for earthquakes of Mt. Etna, on the basis of the strong attenuation of macroseismic intensities (Barbano *et al.*, 2002; Az-zaro, Barbano, *et al.*, 2006).

We believe that the anomalously large low-frequency content of volcanic events played an important role on the high damage level. This belief, which is discussed in the Appendix, is consistent with the highest damage suffered by

Table 2
Comparison between Observed and Predicted PGAs and PGVs

Date (yyyy/mm/dd)	Time (hr:min:sec)	Station	M_L	Distance (km)	PGA SP87 (gal)	PGA BS05 (gal)	PGA WA05 (gal)	PGA Observed (gal)	PGV SP87 (cm/sec)	PGV BS05 (cm/sec)	PGV WA05 (cm/sec)	PGV Observed (cm/sec)
2002/10/27	01:28	BRNT	4.3*	19	28	11	6	4	0.9	0.4	0.2	0.7
2002/10/27	01:58	BRNT	4.6*	13	50	37	16	14	1.9	1.3	0.4	2.3
2002/10/27	02:50	BRNT	4.6	17	38	23	11	9	1.4	0.8	0.3	1.5
2002/10/27	02:50	CATA	4.6	27	25	9	5	4	0.9	0.3	0.2	1.6
2002/10/29	10:02	CATA	4.4	18	32	14	8	15	1.1	0.5	0.2	4.5
2002/10/29	16:39	CATA	4.1	16	28	11	7	6	0.9	0.3	0.1	0.9

Local magnitudes are from the MedNet catalog, when available, or synthesized from strong-motion accelerograms (asterisk).

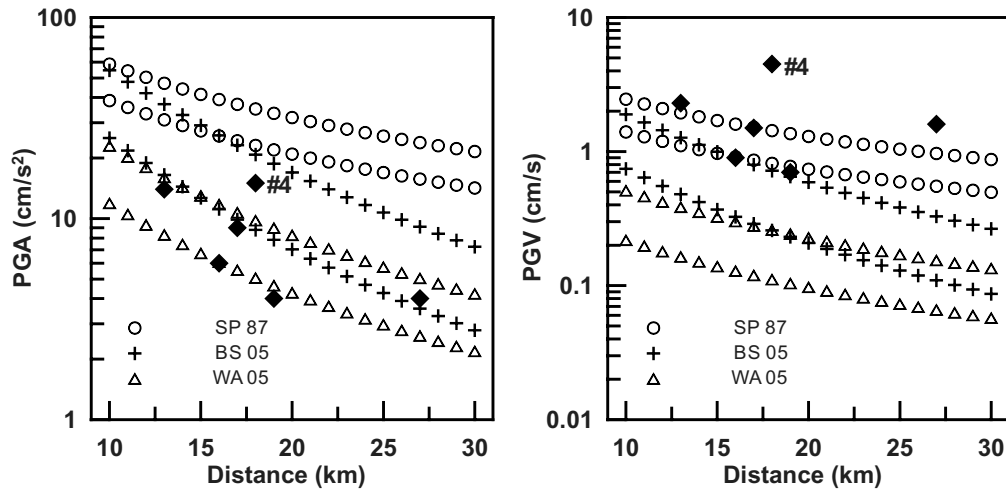


Figure 4. Comparison of observed PGA and PGV values with the empirical regression laws by Sabetta and Pugliese (SP87), Bragato and Sleiko (BS05), and Wald *et al.* (WA05). Upper and lower curves of each regression refer to M_L 4.6 and 4.1, respectively. Note that event 4 is the most damaging earthquake.

systems (i.e., the façades of the churches and ≥ 3 -story reinforced concrete buildings) characterized by fundamental vibration periods larger than that of low-rise masonry and reinforced concrete buildings, which exhibited a lower level of damage (Goretti and De Sortis, 2003).

Moreover, for these earthquakes, the predominant amplitude in the long-period (LP) band makes the local magnitude estimation misleading: the low-frequency cutoff at 1.25 Hz in the Wood–Anderson response causes a strong underestimation of the real strength of ground motion. Therefore, M_L is not the most suitable magnitude scale to be used for volcanic earthquakes when the predominant spectral content moves down to frequencies $f < 1.25$ Hz. Also, moment magnitude derived from the CMT inversion is not appropriate because the spectral bump is significant for periods $1 < T < 10$ sec but seems to not affect the longer periods ($T > 30$ sec) where the moment tensor inversion is made. For long-period events, the duration-magnitude relationships are not adequate because they are not calibrated over this type of volcanic event (D’Amico and Maiolino, 2005).

Weak Motions

Stations in the Santa Venerina area (Fig. 1) confirm that smaller sized events of the swarm are characterized by the same LP character of the largest events. Figure 7 shows two example seismograms recorded by the same station (SVN4) at short ($R < 10$ km) epicentral distances. Of the two earthquakes, one (event 15) is characterized by a high-frequency spectral content, where P and S waves are clearly visible: it could be classified as a VT-A type, according to the conventional definition of earthquakes in volcanic areas (Wassermann, 2002). The other one (event 7) shows an intermediate behavior between VT-B and hybrid type where body waves are weakly emergent and an LP component predominates in amplitude. The two events have close epicenters but

differ in terms of source depth: 7 and 2 km, respectively (H. Langer, personal communication, 2007).

Although the two earthquakes of Figure 7 attained approximately the same peak ground velocity and are at a similar epicentral distance, their Fourier amplitude spectra show a very different shape. The VT-A event is well fit by a Brune spectrum with a stress drop of 40 bars, attenuated according to Scognamiglio *et al.* (2005). The hybrid event shows spectral amplitudes at 1 Hz that are a factor of 30 larger than those of the VT-A earthquake. This corresponds to a difference by a factor of about 12 in terms of observed peak ground displacements. In contrast, high frequencies are drastically depleted. Peak ground accelerations of the VT-A event exceed those of the VT-B event by a factor between 4 and 5. Low amplitudes at high frequencies could be a source property of volcanic earthquakes but could also be due to the shallower propagation: Q tomography indicates the presence of a 2 km thick, highly attenuating topmost layer in the southeastern flank of Mt. Etna (De Gori *et al.*, 2005). Figure 8 shows the spectra of events 6 to 16 of Table 1. All of the events other than 15 have the predominant spectral content in the low-frequency band ($f < 2$ Hz) deviating significantly from the source scaling of VT-A events. However, it has to be noted that, for $M_L < 4$, the spectral content does not move toward frequencies much lower than 1 Hz; therefore, the M_L underestimation bias is not as significant as it is for the $M_L > 4$ events.

Can Damaging Volcanic Earthquakes Be Recognized in Near-Real Time?

A consolidated magnitude scale like the Richter one is difficult to be replaced: seismic moment inversion is rarely successful for $M_w < 5$, and the available duration-magnitude scale is not applicable to LP events. However, the aforementioned limitations suggest that new criteria, not based on M_L ,

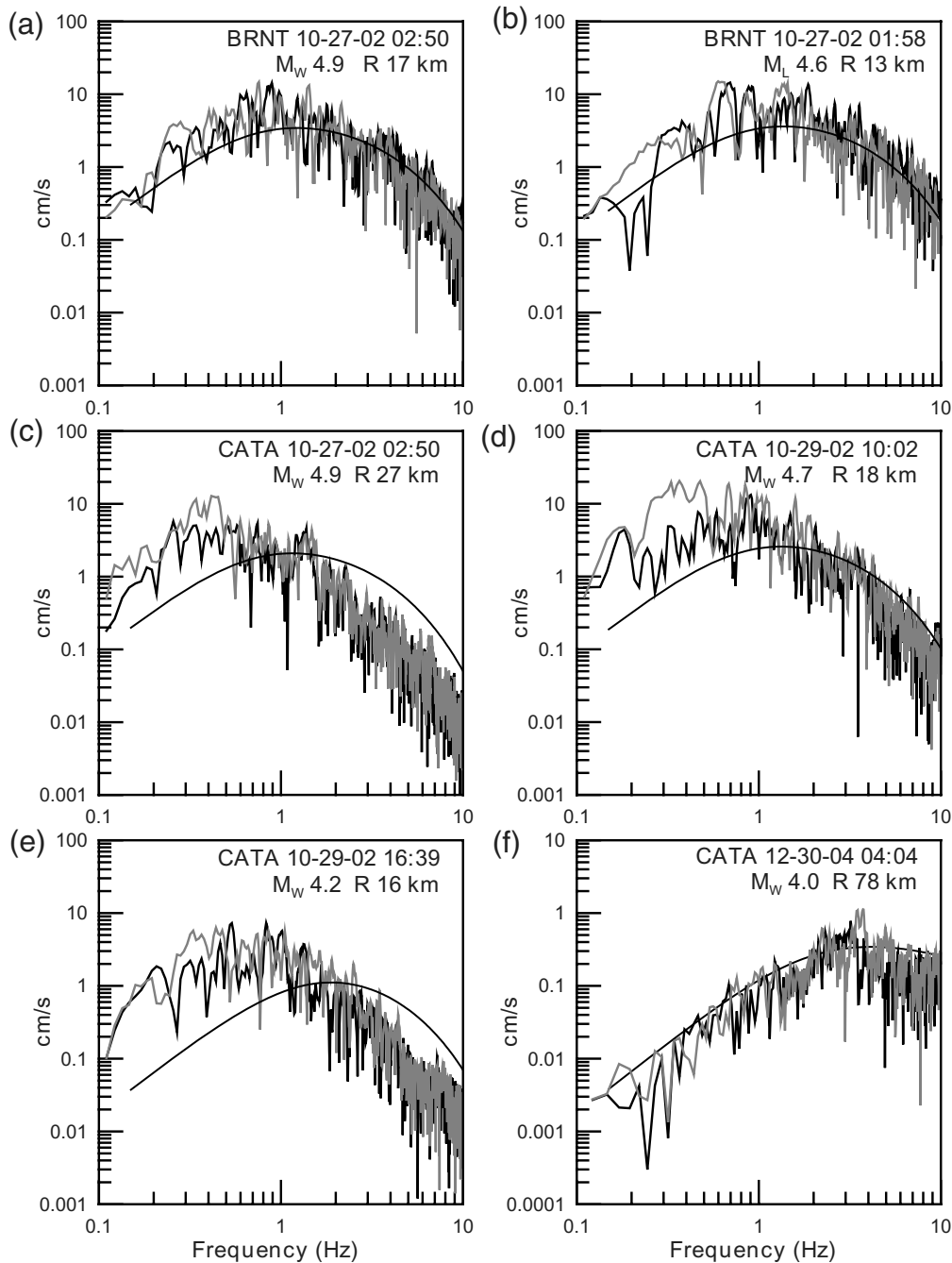


Figure 5. Fourier amplitude spectra of the two horizontal components of ground acceleration: (a)–(e) volcanic events of the October 2002 swarm and (f) tectonic event of 30 December 2004 in the Hyblean Foreland. The smooth curves are theoretical Brune spectra attenuated to the recording sites according to Scognamiglio *et al.* (2005).

have to be found to recognize damaging earthquakes in near-real time. To this purpose, this is the question to which we have to find an answer: is there a way to get an objective ground-motion parameter representative of potential damage a few minutes after the occurrence of a volcanic earthquake? Nowadays, PGV is the most promising ground-motion parameter to be used as a damage indicator (e.g., Akkar and Özen, 2005) and is also currently applied in the generation of ShakeMaps (Wald *et al.*, 1999, 2005).

We checked the reliability of PGV-equivalent magnitude in the case of LP volcanic events (Table 2). The magnitude values obtained using the relationship by Wald *et al.* (2005), although able to produce damage, overestimate real epicentral intensities, as discussed later on. This is not surprising if we take into account the shift in frequency shown in Figure 6 that makes the scaling law of tectonic events to LP volcanic events not immediately applicable. The conclusion is that consolidated damage estimators used for tectonic events can

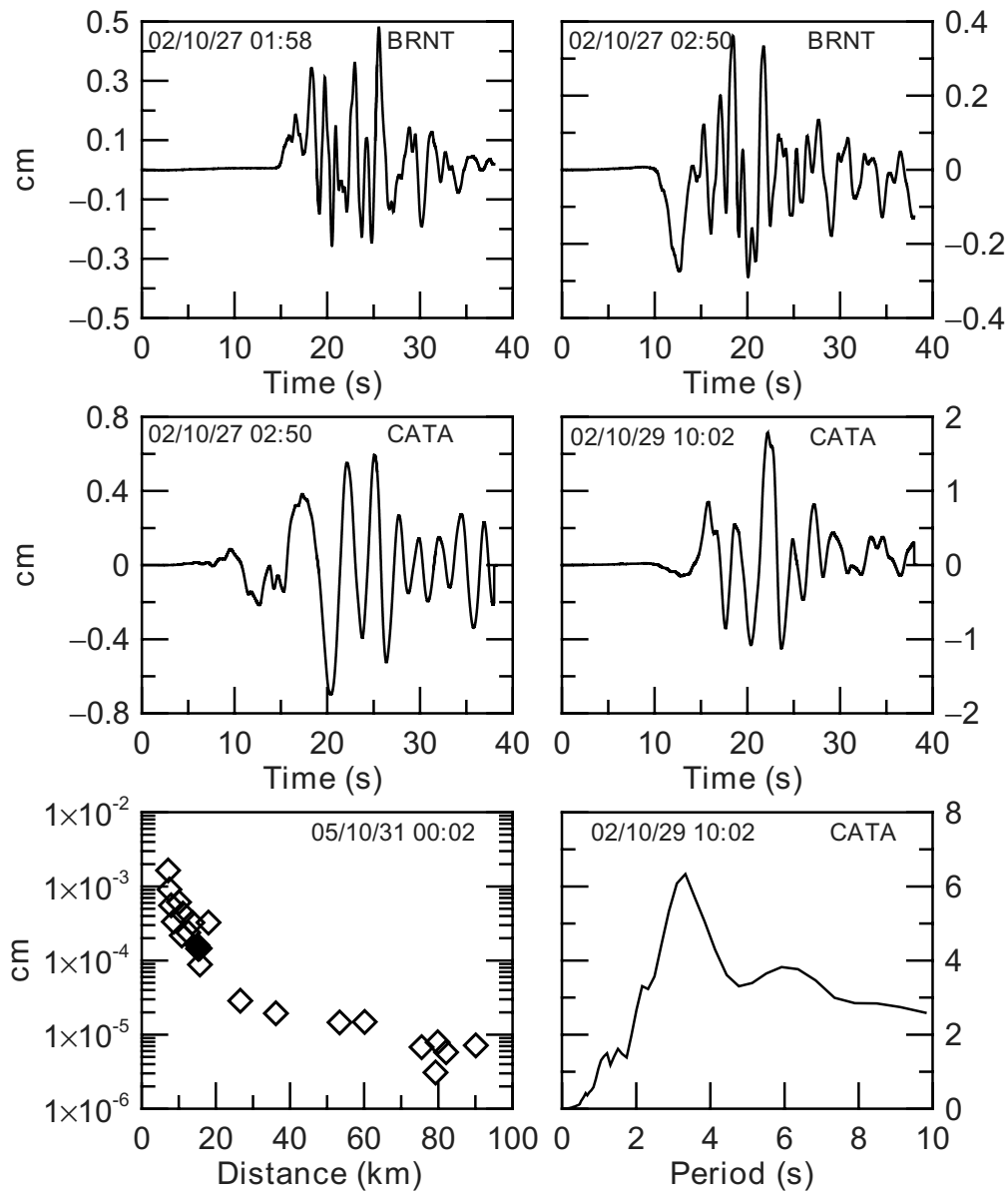


Figure 6. (a)–(d) Time histories of ground displacement (east–west components) of the strongest events of the October 2002 swarm at distances of 13–27 km. Peak ground displacement (PGD) at CATA was as large as 1.8 cm, but likely attained significantly larger values in the damaged zone. Panel (e) shows an example of the usually observed sharp amplitude decay in the epicentral area during a collocated M_L 3.5 tectonic earthquake of 31 October 2005 that was well recorded by INGV stations in Sicily (courtesy of Alessandro Amato and Alessandro Bonaccorso). The black diamond is the PGD of CATA. Panel (f) represents displacement spectral ordinates of the record in panel (d).

give qualitative indications, but a more specific criterion has to be found taking into account the spectral peculiarity of LP volcanic events. We propose a method based on response spectra computation that could be implemented to be routinely used with real-time recordings. Figure 9 shows a 5%-damped pseudovelocity response spectra for some of the strongest of the October 2002 earthquakes. In the same figure, statistical expectations for tectonic earthquakes based on the Sabetta and Pugliese (1996) regression (hereafter denoted as SP96) are also shown. Again, there is a significant (up to a factor of 3) depletion in the observed high-frequency

response spectra compared to the expected curves of SP96. In contrast, at low frequency, response spectra computed from the local recordings are fit by spectral ordinates statistically corresponding to M_L 5.5–6 of tectonic earthquakes in Italy. Figure 9 indicates that the frequency band 0.3–1.5 Hz gives the largest contribution to the pseudovelocity response spectra of volcanic events of Mt. Etna. For a given earthquake and a given epicentral distance R , it is simple to determine the magnitude that, in the SP96 regression, would attain the same spectral ordinates in that frequency band. This is accomplished by constructing a theoretical curve

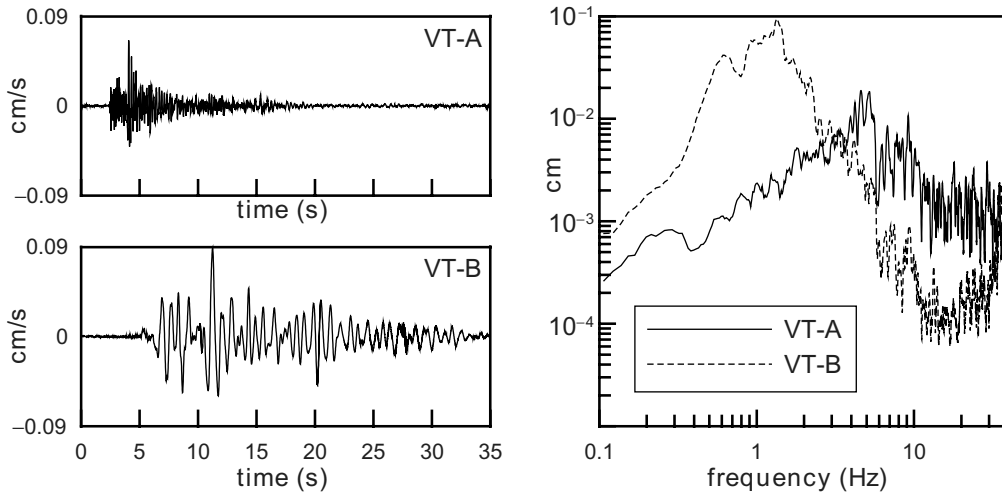


Figure 7. Weak motions for two events of the 2002 swarm recorded in the village of Santa Venerina: note the opposite behavior of low and high frequencies between VT-A and VT-B events.

of the Housner (1952) spectral intensity

$$H(M, R) = \int_{0.5}^{2.5} \text{PSV}_{M,R}(T) dT, \quad (1)$$

where $\text{PSV}_{M,R}(T)$ is the statistical expectation of the 5%-damped pseudovelocity response spectra as a function of period T . According to SP96, we write:

$$\log \text{PSV}_{M,R}(T) = a(T) + b(T)M - \log \sqrt{R^2 + h^2(T)}, \quad (2)$$

where $a(T)$, $b(T)$, and $h(T)$ are the coefficients of the SP96 regression. In equation (2), M is the event local magnitude. Taking into account the peculiarity of volcanic events, the original lower limit of integration proposed by Housner (1952), that is, 0.1 sec, was changed to 0.5 sec in order to

better fit the behavior of medium to high-rise buildings (see the Appendix). In Figure 10, examples of the theoretical curve $H(M, R)$ are intersected by the value of the Housner spectral intensity (horizontal straight line) computed from the accelerograms of the volcanic earthquakes of the October 2002 swarm. As expected on the basis of the fit shown in Figure 9, the values of the Housner spectral intensity computed from records of volcanic earthquakes (diamonds) are significantly larger than the statistical expectation of tectonic earthquakes at the same magnitude and distance. The diamond abscissa corresponds to the local magnitude of each event. Solid diamonds indicate M_L synthesized from the same accelerograms used to compute the Housner spectral intensity; open diamonds are M_L values taken from the Med-Net catalog when available. In each panel of Figure 10, the intersection of the horizontal straight line with the theoretical Housner curve indicates the magnitude of the earthquake

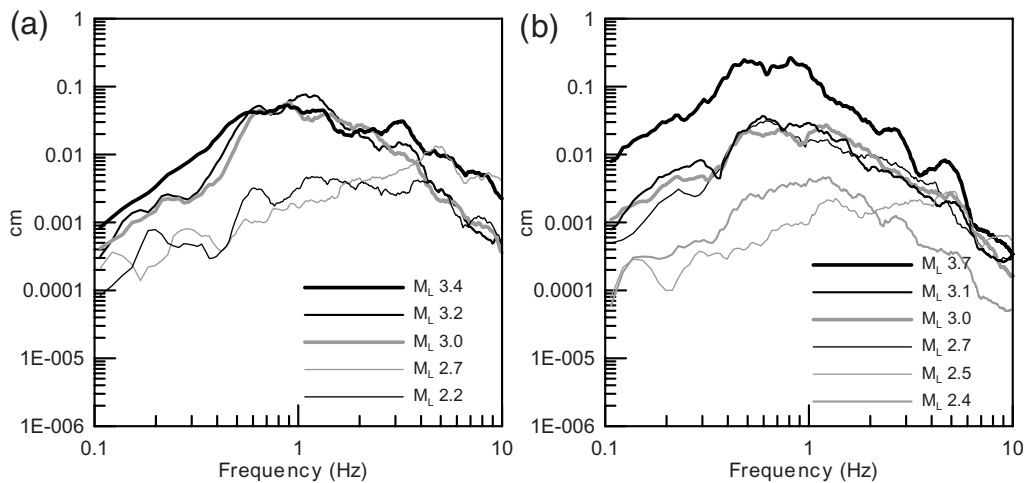


Figure 8. Fourier amplitude spectra of smaller magnitude earthquakes of the 2002 swarm [(a) events of the northeast sector and (b) events of the south-southeast sector].

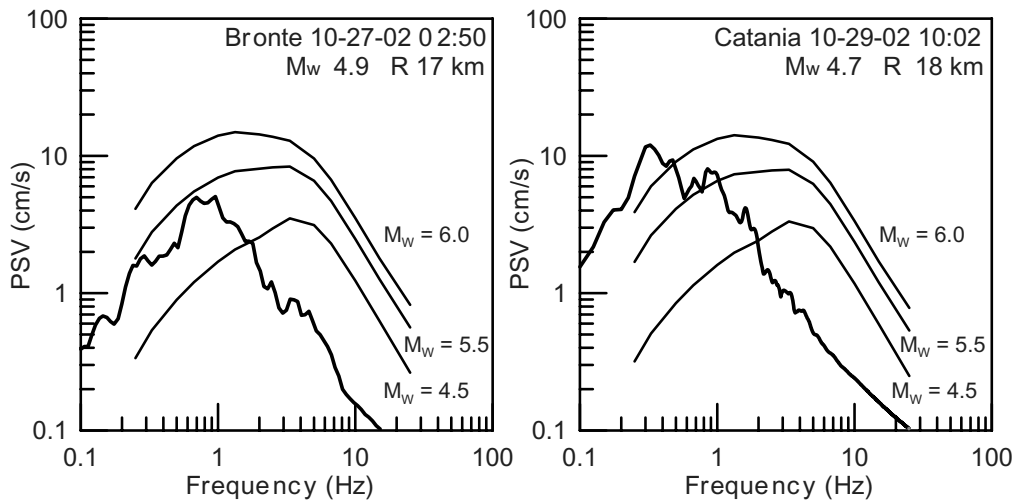


Figure 9. Pseudovelocity response spectra of the strongest events of October 2002, evaluated for M_w 4.5, 5.5, and 6.0, compared to predictions of the Sabetta and Pugliese (1996) regression.

having, in the SP96 regression, the same damage potential. In the case of the event of October 27 (event 3 in Table 1), the computed Housner intensity corresponds to a magnitude of 5.1 (BRNT) and 5.2 (CATA), respectively, while for the October 29 event (4), the Housner intensity attains a magnitude of 5.7 (CATA).

For volcanic LP earthquakes, the use of the magnitude inferred from equation (1) leads to a preliminary indication of the epicentral macroseismic intensity (I_0) that is urgently required by the civil protection authorities. This estimate is more realistic than the one using regressions versus instrumental magnitude or other estimators of intensity (PGV, etc.). Figure 11 shows the magnitude-maximum intensity curve assessed by Di Filippo and Marcelli (1950). This is the relationship conventionally used in Italy for a statistical determination of the maximum intensity as soon as an earthquake occurs. For the 29 October 2002 earthquake, we obtain a value of 5.7 using the magnitude abscissa inferred from the Housner intensity. As shown in Figure 11, this would have predicted a maximum intensity of VIII–IX, which differs by less than one degree from the experienced $I_0 = \text{VIII}$ (Azzaro, D’Amico, *et al.*, 2006), whereas the instrumental M_L value (4.4) would correspond to intensity VI–VII. As discussed in the Appendix, in the epicentral area medium to high-rise reinforced concrete (RC) buildings exhibited a higher level of damage (corresponding to $I = \text{VIII}$) with respect to masonry buildings (corresponding to $I = \text{VI–VII}$). This circumstance can be explained with the low-frequency content of the causative earthquake. Thus, a significant discrepancy between instrumental and Housner-derived magnitude could be a quick indicator of the aforementioned effect.

Other intensity-magnitude correlations exist that have been specifically computed for shallow volcanic earthquakes (e.g., Barbano *et al.*, 2002; Azzaro, Barbano, *et al.*, 2006). They would have yielded a high intensity as well. However, *a priori* it is not obvious what regression is the best one to be

used just after an earthquake. Moreover, volcanic-earthquake relations make use of duration magnitude, and this does increase uncertainties since duration-magnitude suffers the lack of an appropriate calibration for LP events. In contrast, the proposed method to assess I_0 is based on a quantification of elastic structure vibrations excited by the recorded ground motions. Therefore, the result is valid independently of the nature of the causative earthquake.

Conclusions

Damaging volcanic earthquakes of the October 2002 swarm were the first ones to be recorded locally by strong-motion instruments in the Mt. Etna area. As already observed in other volcanic areas (Jousset and Douglas, 2007, and references therein) strong-motion accelerograms and weak-motion seismograms are characterized by an enrichment of long-period (1–10 sec) motions, compared to tectonic earthquakes of equivalent magnitude. Our study shows that a depletion in amplitude at high frequencies is observed as well. These two features imply that (1) conventional source scaling of tectonic earthquakes does not fit the ground motions of volcanic LP earthquakes, (2) commonly used magnitude scales are not adequate for volcanic LP earthquakes, as they are not good measures of their maximum shaking, (3) ground displacements of volcanic LP earthquakes at magnitudes of the order of 4 attain amplitudes typical of tectonic earthquakes at magnitudes as large as 5 to 6, and (4) LP events can cause severe damage to long-period structures but even to medium-rise reinforced concrete buildings. Based on statistical regressions of low-frequency pseudovelocity response spectra as a function of magnitude (Sabetta and Pugliese, 1996), a procedure is proposed that computes the spectral ordinates from real-time records and provides magnitude values more usable to assess the potential level of damage in near-real time.

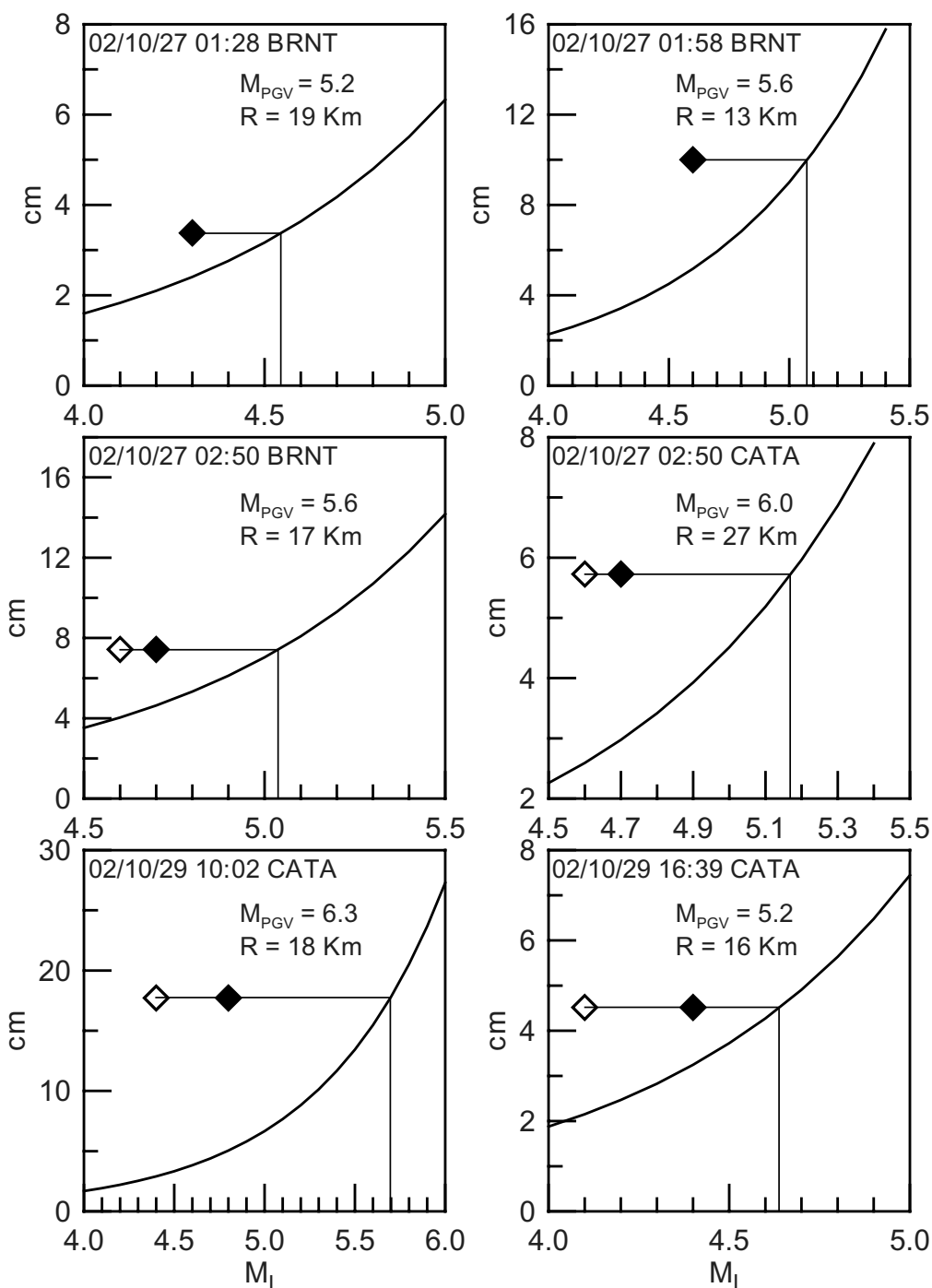


Figure 10. Theoretical curves of the Housner spectral intensity (equation 1) derived from the Sabetta and Pugliese (1996) regression. Housner intensity computed using the local accelerograms is represented by diamonds (open and solid diamonds correspond to Mednet M_L estimates and values synthesized from accelerograms, respectively). Intersection between horizontal and vertical straight lines gives the magnitude of a tectonic event with the same Housner intensity in the 0.5–2.5 sec integration interval.

Data and Resources

Strong-motion records from the BRNT and CATA stations can be obtained from the Italian Accelerometric Archive at <http://itaca.mi.ingv.it> (last accessed in May 2008). Weak-motion data are part of an experiment carried out by the Istituto Nazionale di Geofisica e Vulcanologia (INGV)

(Roma1, Seismology and Tectonophysics Section) and are available upon request to the authors.

Acknowledgments

This work has been carried out with internal research funds of the INGV. Some investigations are also part of the Italian Seismological Project

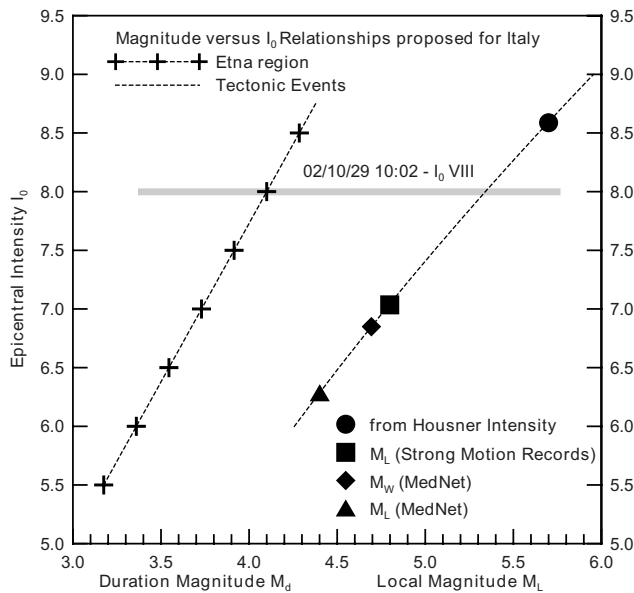


Figure 11. Maximum intensity-magnitude relationships of volcanic and tectonic earthquakes in Italy. The prediction of the epicentral macroseismic intensity of volcanic earthquakes is improved by using the magnitude values derived from the statistical relationship between pseudovelocity response spectra and moment magnitude of tectonic earthquakes (Sabetta and Pugliese, 1996).

S5 (Definizione dell'input sismico sulla base degli spostamenti attesi) of the 2005–2007 Dipartimento Protezione Civile—Istituto Nazionale di Geofisica e Vulcanologia research programs. We are grateful to Julian Bommer and Steve Malone for a thorough and constructive revision of a previous version of the text, which significantly helped us in improving the manuscript. We also thank Dave Boore for criticism and useful suggestions.

References

- Akkar, S., and Ö. Özgen (2005). Effect of peak ground velocity on deformation demands for SDOF systems, *Earthq. Eng. Struct. Dyn.* **34**, 1551–1571.
- Azzaro, R., M. S. Barbano, S. D'Amico, and T. Tuvè (2006). The attenuation of seismic intensity in the Etna region and comparison with other Italian volcanic districts, *Ann. Geophys.* **49**, 1003–1020.
- Azzaro, R., S. D'Amico, A. Mostaccio, L. Scarfi, and T. Tuvè (2006). Terremoti con effetti macrosismici in Sicilia orientale nel periodo gennaio 2002–dicembre 2005, *Quad. Geofis.* **41**, 62, Istituto Nazionale di Geofisica e Vulcanologia, Rome, Italy (in Italian).
- Barbano, M. S., M. Cosentino, and G. Lombardo (2002). Intensity attenuation law in the eastern flank of Mt. Etna, in *Proceedings of the Workshop on Seismic Phenomena Associated with Volcanic Activity*, European Seismological Commission, Montserrat, West Indies.
- Barberi, G., O. Cocina, V. Maiolino, C. Musumeci, and E. Privitera (2004). Insight into Mt. Etna (Italy) kinematics during the 2002–2003 eruption as inferred from seismic stress and strain tensors, *Geophys. Res. Lett.* **31**, L21614, doi 10.1029/2004GL020918.
- Bazzurro, P., F. Mollaioli, A. De Sortis, and S. Bruno (2006). Effects of masonry walls on the seismic risk of reinforced concrete frame buildings, in the *Proceedings of 8th US National Conference on Earthquake Engineering*, San Francisco.
- Bommer, J. J., R. Pinho, and H. Crowley (2006). Using a displacement-based approach for earthquake loss estimation, in *Advances in Earthquake Engineering for Urban Risk Reduction*, NATO Science Series, Vol. **66**, Springer, New York, 489–504.
- Boore, D. M., and J. J. Bommer (2005). Processing strong-motion accelerograms: needs, options and consequences, *Soil Dyn. Earthquake Eng.* **25**, 93–115.
- Braga, F., M. Dolce, and D. Liberatore (1982). Southern Italy November 23, 1980 earthquake: a statistical study on damaged buildings and an ensuing review of the M.S.K.-76 scale, Consiglio Nazionale delle Ricerche, Progetto Finalizzato Geodinamica Report No. 503, Rome, Italy.
- Braga, F., M. Dolce, and D. Liberatore (1985). A statistical study on damaged buildings and an ensuing review of the M.S.K.-76 scale, in the *7th European Conference on Earthquake Engineering*, Athens, Greece.
- Bragato, P. L., and D. Slejko (2005). Empirical ground-motion attenuation relations for the Eastern Alps in the magnitude range 2.5–6.3, *Bull. Seismol. Soc. Am.* **95**, 252–276.
- Brune, J. (1970). Tectonic stress and the spectra of seismic shear waves from earthquakes, *J. Geophys. Res.* **75**, 4997–5009.
- Building Seismic Safety Council (1997). National Earthquake Hazards Reduction Program (NEHRP) guidelines for the seismic rehabilitation of buildings, Federal Emergency Management Agency (FEMA) Report No. 273, developed by the Applied Technology Council for FEMA, Washington, D.C.
- Comartin, C. D., and R. W. Niewiarowski (1996). Seismic evaluation and retrofit of concrete buildings, Applied Technology Council Report No. SSC 96-01.
- D'Amico, S., and V. Maiolino (2005). Local magnitude estimate at Mt. Etna, *Ann. Geophys.* **48**, 215–229.
- De Gori, P., C. Chiarabba, and D. Patanè (2005). Q_p structure of Mount Etna: constraints for the physics of the plumbing system, *J. Geophys. Res.* **110**, B05303, doi 10.1029/2003JB002875.
- Di Filippo, D., and L. Marcelli (1950). Magnitudo ed energia dei terremoti in Italia, *Ann. Geofis.* **3**, 337–355.
- Dipartimento Protezione Civile (2002). Rapporto finale della Commissione per l'aggiornamento dell'inventario e della vulnerabilità degli edifici, Rome, Italy (in Italian).
- Fajfar, P. (1999). Capacity spectrum method based on inelastic demand spectra, *Earthq. Eng. Struct. Dyn.* **28**, 979–993.
- FEMA-356 (2000). *Prestandard and Commentary for the Seismic Rehabilitation of Buildings*, Federal Emergency Management Agency, Redwood City, California.
- FEMA-440 (2005). *Improvement of Nonlinear Static Seismic Analysis Procedures*, Federal Emergency Management Agency, Redwood City, California.
- Goretti, A., and A. De Sortis (2003). Il danneggiamento dovuto al sisma etneo del 29 Ottobre 2002, *Ing. Sismica* **20**, 12–20 (in Italian).
- Grunthal, G. (1998). European Macroseismic Scale 1998, *Cah. Cent. Eur. Geodyn. Deism.* **15**, 1–99.
- Housner, G. W. (1952). Spectrum intensities of strong motion earthquakes, in the *Proceedings of the Symposium of Earthquake and Blast Effects on Structures*, Earthquake Engineering Research Institute, Los Angeles, California, 21–36.
- Istituto Nazionale di Statistica (2001). *14° Censimento generale della popolazione e delle abitazioni 2001*, Rome, Italy (in Italian).
- Jousset, P., and J. Douglas (2007). Long-period earthquake ground displacements recorded on Guadeloupe (French Antilles), *Earthq. Eng. Struct. Dyn.* **36**, 949–963.
- Patanè, D., G. Barberi, O. Cocina, P. De Gori, and C. Chiarabba (2006). Time resolved seismic tomography detects magma intrusions at Mt. Etna, *Science* **313**, 821–823.
- Pondrelli, S., A. Morelli, and G. Ekström (2004). European-Mediterranean regional centroid moment tensor catalog: solutions for years 2001 and 2002, *Phys. Earth Planet. Interiors* **145**, 127–147.
- Regione Siciliana (2002). *Usability Inventory* (database file), Palermo.
- Richter, C. F. (1958). *Elementary Seismology*, W. H. Freeman, San Francisco, 768 pp.
- Sabetta, F., and A. Pugliese (1987). Attenuation of peak horizontal acceleration and velocity from Italian strong-motion records, *Bull. Seismol. Soc. Am.* **77**, 1491–1513.

- Sabetta, F., and A. Pugliese (1996). Estimation of response spectra and simulation of nonstationary earthquake ground motions, *Bull. Seismol. Soc. Am.* **86**, 337–352.
- Scognamiglio, L., L. Malagnini, and A. Akinci (2005). Ground-motion scaling in eastern Sicily, Italy, *Bull. Seismol. Soc. Am.* **95**, 568–578.
- Wald, D. J., V. Quitoriano, T. H. Heaton, and H. Kanamori (1999). Relationships between peak ground acceleration, peak ground velocity, and Modified Mercalli intensity in California, *Earthq. Spectra* **15**, 557–564.
- Wald, D. J., B. C. Worden, V. Quitoriano, and K. L. Pankow (2005). ShakeMap manual: technical manual, user's guide, and software guide, in Book 12, Section A, Chapter 1 of *U.S. Geological Survey Techniques and Methods*, U.S. Geological Survey, Reston, 132 pp.
- Wassermann, J. (2002). Volcano seismology, in *New Manual of Seismological Observatory Practice (NMSOP)*, International Association of Seismology and Physics of the Earth's Interior (IASPEI), P. Bormann (Editor), GeoForschungsZentrum, Potsdam.

Appendix

Several displacement-based approaches are available in the literature for earthquake damage estimation (Bommer *et al.*, 2006). The procedure reported hereafter does not account for probabilistic uncertainties in the parameters involved; it can be intended as an effective tool for explaining differential damage observed on reinforced concrete buildings in the study area.

It is well accepted that the maximum top displacement of a reinforced concrete building (multidegree-of-freedom system [MDOF]) can be calculated using an equivalent single-degree-of-freedom system (SDOF), having the stiffness k^* corresponding to the first branch secant stiffness of the load-displacement curve of the building and a suitable "equivalent" mass,

$$m^* = \sum m_i \Phi_i, \quad (\text{A1})$$

where m_i is the i th story mass and Φ_i is the corresponding displacement shape. The displacement shape Φ_i approximates the seismic response of the MDOF (Fajfar, 1999). Thus, the fundamental vibration period of the SDOF can be calculated,

$$T^* = \sqrt{\frac{k^*}{m^*}}, \quad (\text{A2})$$

and the maximum seismic displacement can be obtained from the displacement response spectrum. The top displacement of the MDOF can be estimated by multiplying the maximum SDOF displacement by the modal participation factor Γ :

$$D_{\text{MDOF}} = \Gamma D_{\text{SDOF}}, \quad (\text{A3})$$

where Γ is defined as

$$\Gamma = \frac{\sum m_i \Phi_i}{\sum m_i \Phi_i^2}. \quad (\text{A4})$$

The aforesaid approach can be applied to explain a different behavior observed, during the October 2002 swarm, between

low- and medium-rise reinforced concrete buildings. We consider two- and four-story buildings as representative of the two categories, respectively. In the engineering practice, the effective fundamental vibration period of a SDOF, equivalent to a four-story reinforced concrete building, and the modal participation factor can be estimated as 1.0 and 1.4 sec, respectively (Comartin and Niewiarowski, 1996; FEMA-356, 2000). If we consider the displacement response spectrum of the east–west components of the CATA station for event 4, the spectral displacement at 1 sec is about 1 cm, while the peak ground displacement (PGD) for the same component is 1.8 cm (Fig. 6). The ratio η between the spectral displacement at 1 sec (D_{SDOF}) and the PGD is about 0.6:

$$D_{\text{SDOF}} \sim \eta \text{PGD}. \quad (\text{A5})$$

As discussed before, we have assessed that the horizontal ground displacement did attain amplitudes as large as 15 cm in the epicentral area; thus, a four-story reinforced concrete building could have experienced a top displacement:

$$D_{\text{MDOFM}} = \Gamma D_{\text{SDOF}} \sim \Gamma \eta \text{PGD} \sim 13 \text{ cm}. \quad (\text{A6})$$

For reinforced concrete buildings a good correlation is found between the level of seismic damage and the maximum drift ratio δ_{max} , that is, the maximum ratio between the relative horizontal displacement between two floors and the story height (Building Seismic Safety Council, 1997). Another commonly used parameter is the top drift ratio δ_{top} , that is, the ratio between the maximum top displacement and the building height H . Because of dynamical effects, the maximum drift ratio can be assumed, on average, to be 40% greater than the top drift ratio (FEMA-440, 1995). With the estimated top displacement of about 13 cm, the top drift ratio for a four-story building, whose height is about $H = 12$ m, is

$$\delta_{\text{top}} = \frac{D_{\text{MDOF}}}{H} \approx 1.1\% \quad (\text{A7})$$

and the maximum drift ratio is

$$\delta_{\text{max}} \approx 1.4 \delta_{\text{top}} \approx 1.5\%. \quad (\text{A8})$$

Several studies have been devoted in the last few years to the damage estimation of reinforced concrete buildings, thus leading to limit values for the maximum drift ratio corresponding to different damage levels. Bazzurro *et al.* (2006) provide limit drift ratios δ_{max} for different building typologies as a function of a parameter (C_y) representing the ratio between the base shear capacity and the weight of the building. Table 4 of Bazzurro *et al.* (2006) indicates, for $C_y = 0.15$, values of 0.25% and 1.9% as associated to incipient damage and incipient collapse, respectively, for reinforced concrete frames with weak infill walls (typical of the observed buildings; see Goretti and De Sortis, 2003). The value $C_y = 0.15$ is derived knowing that reinforced concrete buildings in the area have been designed for $C = 0.07$ with the

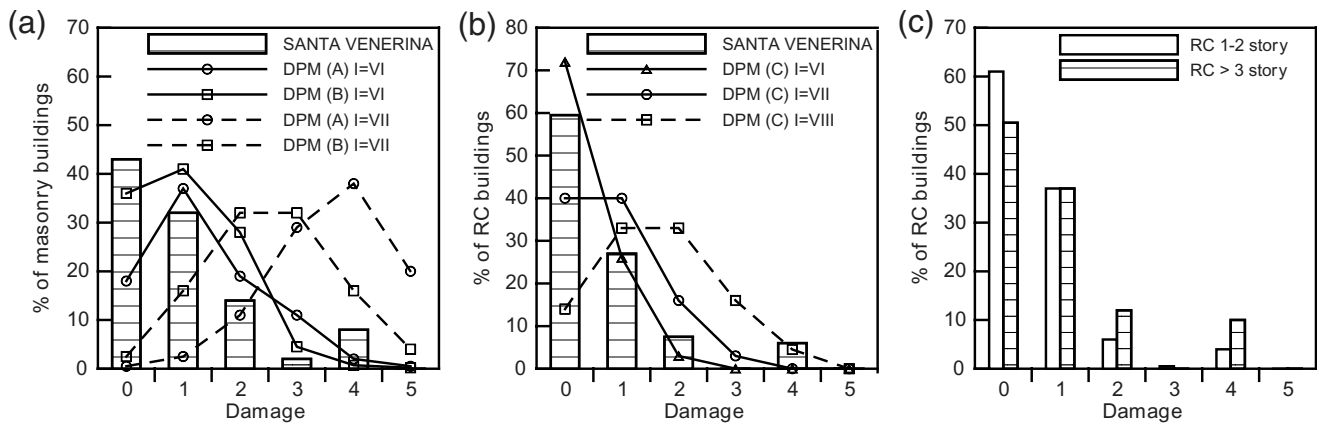


Figure A1. Damage distribution in the municipality of Santa Venerina after the 29 October 2002 earthquake: (a) masonry buildings (total inspected 1606), (b) reinforced concrete (RC) buildings (total inspected 875), and (c) low-rise and medium-rise RC buildings. Dotted, dashed, and solid curves in (a) and (b) show the DPM damage distributions (Braga *et al.*, 1982) for decreasing [from (A) to (C)] levels of seismic vulnerability.

allowable stresses method (C is similar to C_y and corresponds to the ratio between the design resultant lateral loads and the weight of the building). The assumption $C_y \sim 2C$ is based on indications of the former Italian seismic design code. Thus, the maximum drift ratio of 1.5% corresponds to damage ranging from moderate (heavy damage to infill walls and slight damage to reinforced concrete elements) to heavy (disruption of infill walls and heavy damage to reinforced concrete frames): such a level of damage is consistent with observations in the study area (Goretti and De Sortis, 2003).

The aforementioned steps can be repeated for a two-story reinforced concrete building, assuming an effective fundamental vibration period of the equivalent SDOF of 0.5 sec and a modal participation factor Γ of 1.2. In Figure 6, spectral displacement at 0.5 sec is about 0.15 cm, so the ratio between this spectral displacement and the PGD is $\eta = 0.08$; then a top displacement of about 1.5 cm can be estimated using equation (A6). The top drift ratio δ_{top} for this type of building, whose height H is about 6 m, results in 0.25% and the maximum drift ratio δ_{max} is about 0.35% (equation A8). Applying the aforesaid cited limit values, slight damage is obtained; also, such a level of damage is consistent with observations.

The occurrence of selective damage effects seems to be confirmed by the results of a damage and usability survey conducted shortly after the 29 October event (Regione Siciliana, 2002). Figures A1a and A1b show the distribution of masonry and reinforced concrete buildings, respectively, for six damage levels in the municipality of Santa Venerina, where 2500 buildings have been inspected out of 2900 used buildings (Istituto Nazionale di Statistica, 2001). The six levels of damage, approximately consistent with the European Macroseismic Scale (Grunthal, 1998), have been estimated modifying the general framework proposed by the Dipartimento Protezione Civile (2002) in order to highlight the apparent damage.

In the same figure, the damage probability matrix (DPM) damage distributions (Braga *et al.*, 1982, 1985) calibrated for the tectonic Irpinia, southern Italy, 1980 earthquake are also shown. The DPM damage distribution for $I = VI$ for intermediate vulnerability (B) is the most consistent with observations on masonry buildings, with level 4 of damage corresponding to $I = VI-VII$. By contrast, the damage distribution of $I = VII$ for minimum vulnerability (C) is the most consistent with observations on reinforced concrete buildings, with level 4 of damage consistent only with DPM distributions corresponding to intensities as large as $I = VIII$. The macroseismic estimate $I_0 = VIII$ (Azzaro, D'Amico, *et al.*, 2006) has been evidently driven by the huge damage to reinforced concrete buildings.

Furthermore, the differential behavior between low-rise and medium-rise RC buildings, predicted by theory, is confirmed by observations (Fig. A1c).

Istituto Nazionale di Geofisica e Vulcanologia
Via di Vigna Murata 605
00143 Roma, Italy
milana@ingv.it
(G.M., A.R., G.C.)

Dipartimento della Protezione Civile
Via Vitorchiano 2
00189 Roma, Italy
(A.D., P.M.)

Geocheck, Società Responsabilità Limitata
Via della Zagara 83
95045 Misterbianco, Catania, Italy
(G.C., M.C.)